Crystal Growth and The Study of Magnetic Dilution on Kitaev Material α-$RuCl_3$

Ankit Labh

A dissertation submitted for the partial fulfilment
of BS-MS dual degree in Science

Indian Institute of Science Education and Research (IISER) Mohali

May 2018

Certificate of Examination

This is to certify that the dissertation titled **Crystal Growth and The Study of Magnetic Dilution on Kitaev Material α-RuCl$_3$** submitted by **Ankit Labh** (Reg.No. MS13003) for the partial fulfillment of BS-MS dual degree programme of the Institute, has been examined by the thesis committee duly appointed by the Institute. The committee finds the work done by the candidate satisfactory and recommends that the report be accepted.

Dr. Goutam Sheet Dr. Sanjeev Kumar Dr. Yogesh Singh
(Supervisor)

Dated: May, 2018

Declaration

The work presented in this dissertation has been carried out by me under the guidance of Dr.Yogesh Singh at the Indian Institute of Science Education and Research Mohali.

This work has not been submitted in part or in full for a degree, a diploma, or a fellowship to any other university or institute. Whenever contributions of others are involved, every effort is made to indicate this clearly, with due acknowledgement of collaborative research and discussions. This thesis is a bonafide record of original work done by me and all sources listed within have been detailed in the bibliography.

Ankit Labh
(Candidate)

Dated: May, 2018

In my capacity as the supervisor of the candidate's project work, I certify that the above statements by the candidate are true to the best of my knowledge.

Dr.Yogesh Singh
(Supervisor)

Acknowledgements

I would like to thank my supervisor Dr.Yogesh Singh for his kind guidance and all kind of support throughout my project. I learnt and enjoyed a lot in working at his lab. I am deeply indebted to the fellow members of Novel Materials Lab: Anzar, Ashiwini, Kavita, Amit, Jaskaran, Gopal Sir and Shama for helping me in various ways. I thank Mr.Shalender of Ultra Low Temperature Lab for useful discussions and help in many parts of the experiment.

I am grateful to my friends at IISER Mohali- Rupendra, Prabhat, Lalit, Vijay and Avinash, without whom my stay over 5 years can't be imagined. They were part of all crimes and awesome moments throughout these five years. A special thanks to Anamika whose suggestions always worked for me and who helped me out from times of low moral. I acknowledge our library for facilitating and helping me with books and online resources. It also helped me in providing various articles at the time of need and provided me the smart room for career related interviews. I would like to acknowledge our founding director Dr.N.Sathyamurthy for moral support and personal encouragement.

No words will ever suffice to express my gratitude to my parents. They have been my support from the very first day of my born and continue to encourage me, trust me from so far. ...

Contents

List of Figures

Dedicated to Maa . . .

Chapter 1

Introduction

The transition metal halide $RuCl_3$ is well-known material for research in the scientific community, specially for chemists. It has synthesized near a century ago ,and most of the studies on it was based on solution chemistry. In contrast, comparatively less work is done on the part of investigating physical, transport and thermodynamic properties of $RuCl_3$. Physicists started taking interest in α -$RuCl_3$ when Plumb reported that α-$RuCl_3$ could be a good candidate for studying Kitaev Physics[1] in real material. This work results in a series of investigations into the system α-$RuCl_3$.

This was in particular interesting for condensed matter physicists, because Quantum spin liquids(QSLs) are among the most puzzling quantum phases of matter. Kitaev's honeycomb lattice model predicts QSL as its ground state.In these magnetic systems, spin does not order and thus fluctuates strongly even at zero Kelvin. Kitaev Quantum spin liquids(K-QSL) have recently attracted so much attention because of its being an exactly solvable model, which may hosts a variety of different phases.

Ever since the theoretical prediction, numerous quantum spin liquid candidate materials have been synthesized till date and some of the examples include Na_2IrO_3 and Li_2IrO_3. Recently, honeycomb layered α-$RuCl_3$ got much attention from the condensed matter community, since it has structural similarity with Na_2IrO_3 which was a Kitaev candidate. Indeed this too is a K-QSL candidate. In our study, we want to explore the evolution of properties as we tune the material with magnetic dilution.

Soon after the superconducting properties of MgB_2 was found well fitting with two gap model of superconductivity, physicist started looking into the explanation of origin of this behavior. OsB_2 and RuB_2 was soon realized to have properties between those of type-1 and type-2 superconductors. It sparked a interest in searching of new candidates of multi-band superconductors. The superconducting transition of OsB_2 in heat capacity is first order-like in finite magnetic fields, which is a signature of type-1 superconductor while the Ginzburg-Landau parameter κ suggests type-2 behaviour. Earlier, MgB_2 had both kind of superconducting behavior, and it was often termed as type-1.5 superconductor. In this thesis, I have studied the superconducting properties of OsB_2 poly crystals. The parent compound was diluted with Ruthenium at the place of Os and resistivity measurement was done to study superconductive properties.

1.1 The Kitaev's Honeycomb Lattice Model

The Kitaev model is a spin Hamiltonian where spin-1/2 moments sit on a honeycomb lattice with bond-dependent interaction. It was shown by Alexei Kitaev[2] to be exactly solvable with a spin liquid ground state carrying anionic excitations.

It is exactly solvable on any tri-coordinated lattice, independent of lattice geometry and spatial dimension.It's Hamiltonian

$$H_{Kitaev} = -\sum_{\gamma-bonds} J_\gamma {\sigma_j}^\gamma {\sigma_k}^\gamma$$

where $\gamma \in \{x, y, z\}$ labels the j-k bond and J is the exchange interaction depends on the direction of the bond joining the two spins. σ is usual Pauli operators. These models exhibit strong exchange frustration arising from bond directional interactions, which leads to a spin liquid phase[3].Depending on the underlying lattice, the Kitaev model hosts a variety of both gapped and gapless quantum spin liquid phases.

Although the Kitaev's honeycomb lattice model was first suggested to be a purely theoretical model but it was not immediately clear how the Kitaev interaction can be seen in materials. It was the work of Khalliulin[4]which suggests that the crystals made up of octahedrally coordinated transition metal having strong spin-orbit coupling can show spin interactions of this form.

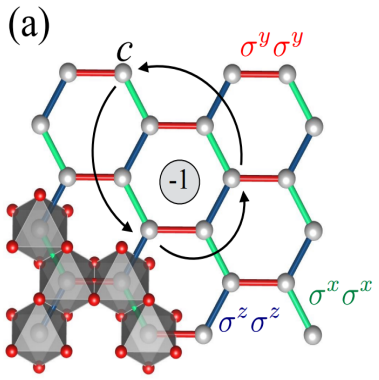

FIGURE 1.1: (a) Kitaev interactions on the honeycomb lattice. The edge-sharing oxygen octahedra are indicated on the left

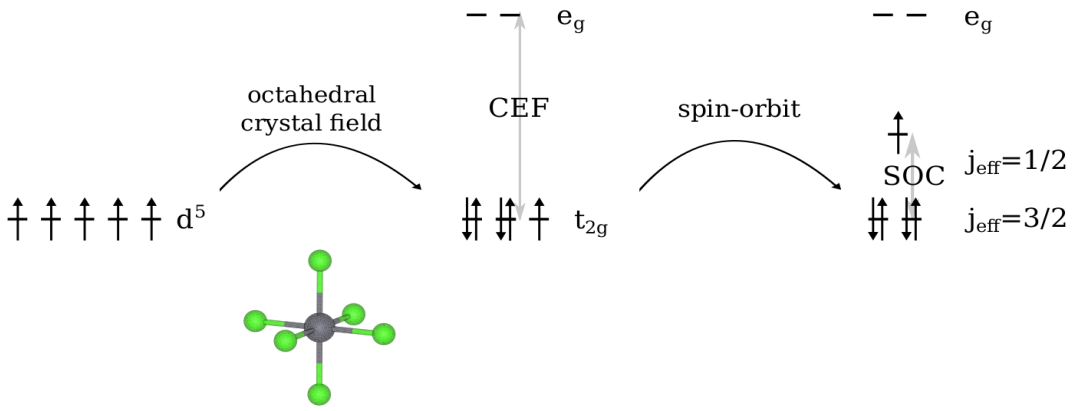

FIGURE 1.2: d orbitals first splits due to octahedral crystal field and then due to spin-orbit coupling. An atom of d^5 configuration will have a hole in t_{2g} orbital giving the effective 1/2 moment must to realize the Kitaev model in a real system[5]

In the Hamiltonian, in addition to Kitaev term, other terms, like the direct exchange between overlapping d orbitals can also be present due to other exchange paths. In materials, if crystal geometry deviates from the octahedral(with 90° angles) then there may be other allowed symmetry terms present in the Hamiltonian. This is not favorable as the presence of new terms will tend to destabilize the spin liquid ground state and may lead to a magnetically ordered system. These perturbing terms are always present in materials but pure Kitaev model spin liquid ground state is stable against small perturbations.

In real materials, Bond-dependent magnetic interaction term has been identified in the sodium iridate[6]. Sodium and Lithium honeycomb iridates order magnetically at low temperature but the ordering is consistent with the presence of significant Kitaev interactions[7–9].

1.2 Electronic State of α-$RuCl_3$

The honeycomb transition metal-halide α-$RuCl_3$ was suggested to be a possible Kitaev material by Plumb et al. in 2014[1] α-$RuCl_3$ crystallizes in the stacked honeycomb lattice with Ru atom at the octahedral site as required for realization of Kitaev model in real materials.

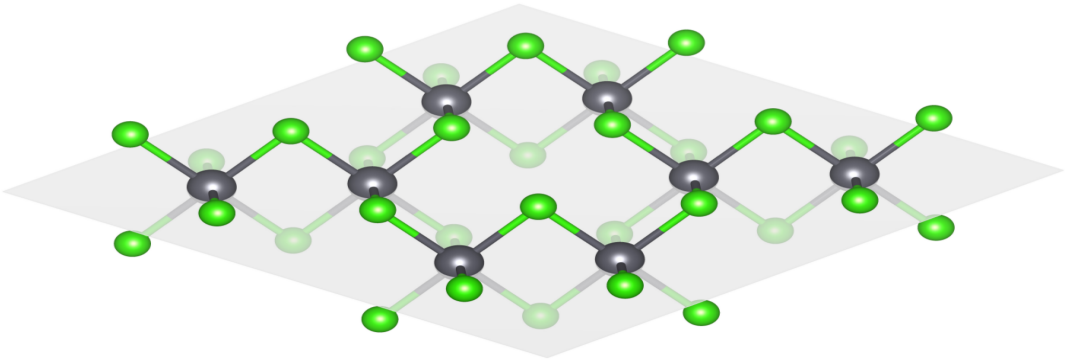

FIGURE 1.3: Crystal structure of metal atoms in octahedral coordination in α-$RuCl_3$[5]

It's lattice is trigonal with space group $P3_121$. In addition to the correct lattice geometry, Kitaev model realization requires Ru atom to be in the appropriate j_{eff} = 1/2 electronic state. Spin-Orbit coupling in Ruthenium atom is smaller than Iridium as it scales as (atomic number)^4. Spin orbit coupling is nevertheless found to be sufficient to split the t_{2g} band.

1.3 Signatures of Kitaev Physics in α-$RuCl_3$

The primary experimental signature for a spin liquid state is the absence of magnetic ordering down to the lowest temperature.. But α-$RuCl_3$ does order magnetically and its ordering temperature is approximately 15K[1, 10] There are some indication that the magnetic Hamiltonian of this material, α-$RuCl_3$, does have a significant Kitaev term.

Banerjee et al. and Cao et al.[11–13] reported inelastic magnetic neutron scattering measurement and detected an unusual broad feature at the centre of Brillouin zone. A sharp magnon is expected in a typical magnetically ordered system but in spite of having ordering at low temperature, it didn't had the sharp magnon which raises the possibility of system being non ordered at low temperature. In

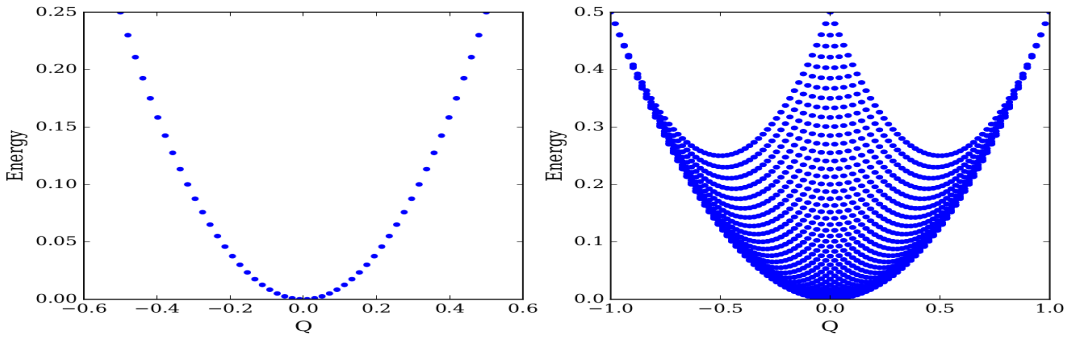

FIGURE 1.4: Single particle dispersion($\omega = Q^2$) and corresponding continuum of two-particle excitations. Schematic demonstrates the continuum that results when two particles are created by the scattered neutrons. The right panel shows the two quasi-particles which are from the single-particle dispersion[5].

their results, a broad continuum of scattering was present at a slightly higher energy of >4meV with respect to lower energy sharp magnon like feature and it persisted well above the ordering temperature too. This kind of continuum had already been reported in Raman scattering[14] These results suggest the presence of fictionalized magnetic excitations which are normally not present in any ordered system but are in accordance with the pure Kitaev term in spin Hamiltonian.

Kitaev's honeycomb lattice model has a remarkable feature that it hosts magnetic excitations that carry fractional quantum numbers. These fractional excitations are seen in inelastic neutron scattering experiment where it results in a broad feature in experiment which is because of the creation of multiple excitations in the material due to scattering particles. The figure shows a simple quadratic dispersion and the continuum of two particles states found by adding momentum and energy to all possible pairs of states from the original dispersion.

The presence of continuum in inelastic neutron scattering suggests of the presence of unusual fractionalized magnetic excitations related to possibly larger Kitaev interaction. So, despite the presence of magnetic order in α-$RuCl_3$, it still exhibits some features of Kitaev spin liquid ground state and thus interesting for physicists to investigate more into it.

Upon recent investigation, in α-$RuCl_3$, Curie-Weiss temperature for ordering within the layer is found to be +32K while in between layers, it is -130K. Energy, temperature and momentum dependence of magnetic excitation in α-$RuCl_3$ are in parallel with the Kitaev honeycomb lattice model. Below 7 K, $RuCl_3$ develops a long range order and above 7 K, the spin fractionalize into localized magnetic fluxes

and itinerant fermions, both of which are composed of majorana fermions. Above ordering temperature, two broad maxima-one around 50K and another around 100K can be seen with a linear temperature dependence between them.

1.4 Superconductivity

Superconductivity is a quantum mechanical phenomenon discovered back in 1911 by Dutch physicist Heike Kamerlingh Onnes.He found it when the electrical DC resistance of a material(mercury) goes to exact zero value. Superconductors also expels out magnetic flux field out of the material when cooled below a characteristic critical temperature known as T_c of the superconductor[15]

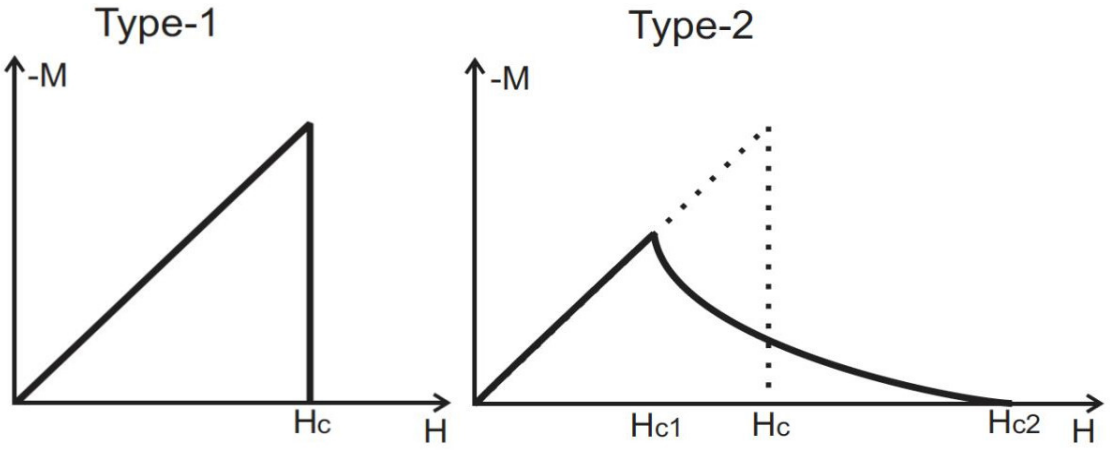

FIGURE 1.5: A comparison of the magnetization in a superconductor versus the applied magnetic field in type I and type II superconductors[17].

A (BCS) superconductor is characterized as either of type-1 or type-2 with respect to the response to a magnetic field. It is called type-1 where there exists just one critical field H_c below which the material is a perfect diamagnet and above which magnetic field lines can penetrate throughout the surface results in lost of superconductivity. It is called type-2 when it has two critical fields H_{c1} and H_{c2}. Below H_{c1}, it is a perfect diamagnet and exhibits Meissner effect while above H_{c2}, superconductivity is lost and the material becomes normal. In between H_{c1} and H_{c2}, magnetic flux can pass through the superconductor by making something called vortex where a localized area of superconductor becomes normal and allows flux quanta to pass through it. Vortices interact with each other and can form a hexagonal lattice.

Microscopic theory of superconductor was given by Bardeen, Cooper and Schrieffer called as BCS theory for which they were awarded noble prize[16]. The theory introduces phonon induced attractive coupling between two electrons and called it cooper pair. So, superconductivity was redefined as the effect caused by condensation of cooper pairs into a boson-like state. Later on new kinds of high temperature superconductors were discovered which was not described by BCS theory.

1.4.1 Meissner Effect

The German physicists Walther Meissner and Robert Ochsenfeld discovered this phenomenon in 1933. According to this, In superconducting state, magnetic field get expels out from the interior of a superconductor which is called Meissner Effect. The Meissner state breaks down when a relatively large magnetic field is applied. Meissner effect is must for something to be called superconductor apart from zero resistance case. It originated due to electric currents called screening currents which flow on the surface of the superconductor generating a field equal and exactly opposite to the applied field. Meissner effect is responsible for the existence of critical field H_c.

1.4.2 BCS Theory

Two electrons of equal and opposite momentum, form a bound state (Cooper pairs) close to Fermi level through the attractive interaction mediated by phonon, leading to a gap in the electronic energy spectrum,Δ , whose magnitude is proportional to the pairing energy scale. These Cooper pairs condense in a phase coherent state which gives the global zero resistance state. This state can be described in terms of a complex order parameter $\Psi^{\iota\theta}$, whose amplitude is proportional to the pairing strength, 2Δ and θ is the phase factor of the condensate. Within BCS theory, the destruction of zero resistance state occurs at the temperature where Δ, and hence Ψ goes to zero. However, in principle, the superconducting (SC) state can also get destroyed through phase fluctuations even when the pairing amplitude remains finite

1.5 Multi-gap Superconductivity

A conventional superconductor near T_c is described by a single order parameter field. Depending upon the value of Ginzburg-Landau parameter κ, superconductors are categorized into two groups. If $\kappa < 1/\sqrt{2}$, then it is called type-1 superconductor and if $\kappa > 1/\sqrt{2}$, it is called type-2[18]

In multi-gap superconductors, superconducting components originate from electronic Cooper pairing in different bands. There are three fundamental length scales: two coherence lengths and and the magnetic field penetration length. As a consequence of the three fundamental length scales, there exists a separate superconducting regime where vortices have attractive long range interaction and repulsive short range interaction and also forms vortex clusters immersed in domains of two-component Meissner state in low magnetic field, surrounded by vortex-less areas. Multi-gap superconductors show vortex formation similar to that seen in Type II superconductors. The difference is that type 1.5 superconductors have non-monotonic vortex interaction. This state is often called semi Meissner state[17].

	Single-component type I	Single-component type II	Multicomponent type 1.5
Characteristic lengths scales	Penetration length λ and coherence length ξ ($\frac{\lambda}{\xi} < \frac{1}{\sqrt{2}}$)	Penetration length λ and coherence length ξ ($\frac{\lambda}{\xi} > \frac{1}{\sqrt{2}}$)	Two characteristic density variations length scales ξ_1,ξ_2 and penetration length λ, the nonmonotonic vortex interaction occurs in these systems typically when $\xi_1 < \sqrt{2}\lambda < \xi_2$
Intervortex interaction	Attractive	Repulsive	Attractive at long range and repulsive at short range
Energy of superconducting/ normal-state boundary	Positive	Negative	Under quite general conditions negative energy of superconductor/ normal interface inside a vortex cluster but positive energy of the vortex cluster's boundary
The magnetic field required to form a vortex	Larger than the thermodynamical critical magnetic field	Smaller than thermodynamical critical magnetic field	In different cases either (i) smaller than the thermodynamical critical magnetic field or (ii) larger than critical magnetic field for a single vortex but smaller than the critical magnetic field for a vortex cluster of a certain critical size
Phases in external magnetic field	(i) Meissner state at low fields (ii) Macroscopically large normal domains at larger fields. First order phase transition between superconducting and normal states	(i) Meissner state at low fields (ii) Vortex lattices/liquids at larger fields. Second order phase transitions between superconducting and vortex states and between vortex and normal states	(i) Meissner state at low fields (ii) "Semi-Meissner state": vortex clusters coexisting with Meissner domains at intermediate fields (iii) Vortex lattices/ liquids at larger fields. Vortices form via a first order phase transition. The transition from vortex states to normal state is second order.
Energy $E(N)$ of N-quantum axially symmetric vortex solutions	$\frac{E(N)}{N} < \frac{E(N-1)}{N-1}$ for all N. Vortices coalesce onto a single N-quantum megavortex	$\frac{E(N)}{N} > \frac{E(N-1)}{N-1}$ for all N. N-quantum vortex decays into N infinitely separated single-quantum vortices quantum vortices	There is a characteristic number N_c such that $\frac{E(N)}{N} < \frac{E(N-1)}{N-1}$ for $N < N_c$, while $\frac{E(N)}{N} > \frac{E(N-1)}{N-1}$ for $N > N_c$. N-quantum vortices decay into vortex clusters.

FIGURE 1.6: A comparison of type 1, type 2 and type 1.5 superconductors[17]

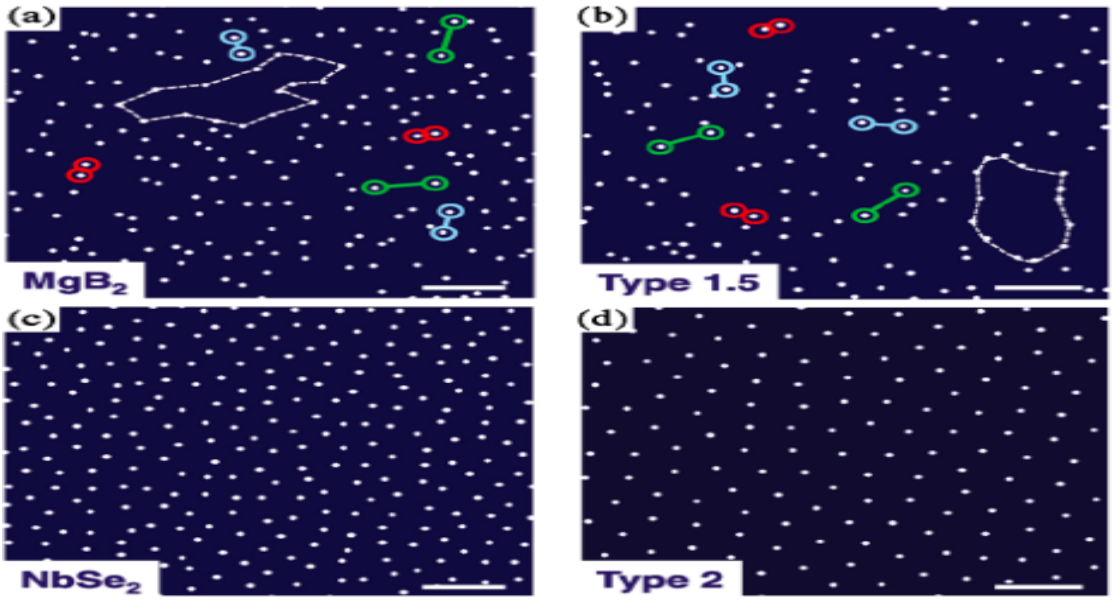

FIGURE 1.7: Vortex cluster formation in Type 1.5 superconductors versus vortex lattice formation in Type II superconductor[19]

Chapter 2

Materials and Growth Methods

For making a crystal of high quality, its constituent must be very pure. We use all the chemicals of high purity either from Sigma Aldrich or Alfa Aesar. We accurately weight chemicals up to the certainty of $\pm$ 0.00001g. We use high-quality quartz tube for sealing.

2.1 Chemicals for Crystal Growth

For $RuCl_3$, box furnace from Nabertherm was used and the sample was vacuum sealed in a quartz tube with V-shape at the end of the tube. Crystals were grown using high purity powders.

OsB_2 and related compounds were made from highly pure Osmium powder(99.95%, Alfa Aesar) and Boron chunks(99.999%, Alfa Aesar) . Os was made pellete using pelletizer. RuB_2 was similarly synthesized using Ru metal powder (99.99%, Alfa Aesar) and Boron chunks (99.999%, Alfa Aesar).

2.2 Box Furnace

A high-temperature box furnace, manufactured by Nabertherm, Germany are used for crystal growths. It has 4 SiC heating elements and can go up to a temperature as high as 1400°C.

FIGURE 2.1: Nabertherm box furnace

2.3 Glove Box

It is very important to preserve the grown samples from the exposure to the unwanted impurities, gases in the atmosphere and sunlight. Since a slight degradation of sample can mask or change the physical properties we are interested to measure. To avoid any contamination from the ambient environment, we have kept our samples in UNIlab Glove Box manufactured by mBraunas as shown in the figure 2.1. The Glove Box is filled with high purity Argon gas (99.99 %) from Sigma, Chandigarh and has a closed gas loop recirculation. It has a purity level $H_2O < 0.1$ ppm, $O_2 < 0.1$ ppm.

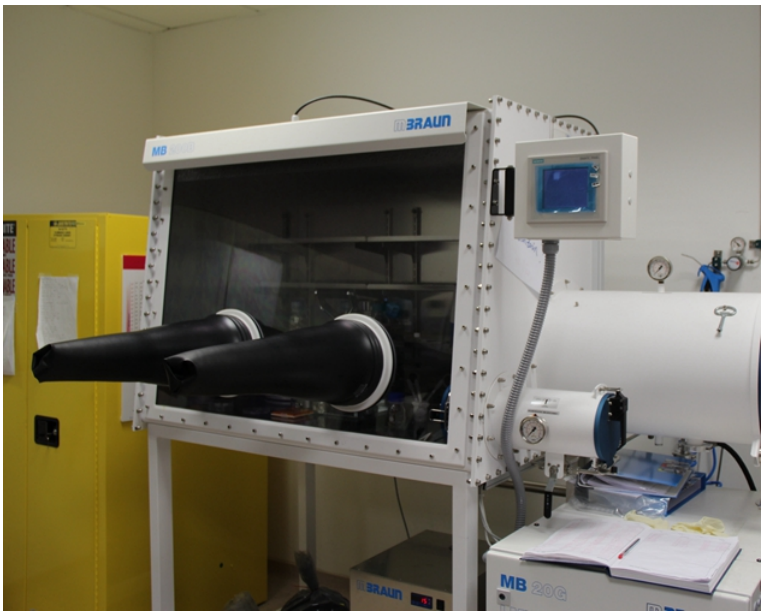

FIGURE 2.2: Glove Box (mBarun)

2.4 Powder X-ray measurement

X-ray diffraction is an essential experimental technique that can give information about the crystal structure of bulk solids, including lattice constants and geometry, the orientation of single crystals, and which includes preferred orientation of polycrystals, defects, stresses, etc. For confirming the phase purity of the polycrystalline samples, we have performed X-ray diffraction by Rigaku Ultima IV fully automatic high-resolution X-ray diffractometer system at the powder x-ray facility, IISER Mohali. Copper was used as the target material with Cu-Kα wavelength of 1.5418Å.

The outcome of XRD spectra are peaks intensity as a function of 2θ. The peak positions of XRD spectra gives unit cell parameters (a, b, c, α, β, γ), symmetry and content. The peak intensity gives atomic parameters (x, y, z etc.), coordinates of atoms and space group symmetry. The peak shape gives information about crystallinity, defects and dislocations in the sample

FIGURE 2.3: Powder XRD (Rigaku)

2.5 Physical Property Measurement System

The PPMS (of Quantum Design) is a fully automated variable temperature and magnetic field system that can measure specific heat, thermal and magneto transport properties of various type of the specimen or samples. Temperatures can be varied from 0.4 K to 400 K and has a magnetic field that can reach up to 9 Tesla. It has many options including VSM and Heat capacity measurement with He-3. It is an Evercool II system, which features an integrated cryocooler-Dewar system that re-condenses and liquefies gaseous helium directly within the EverCool II Dewar. With He-3 setup, it goes down to 0.4 K for heat capacity like measurements otherwise 1.8 K.

FIGURE 2.4: PPMS QD

2.6 Magnetization in SQUID

A SQUID (Superconducting Quantum Interference Device) is a very sensitive magnetometer to measure extremely small magnetic moments. It is based on superconducting loops containing Josephson Junctions. The SQUID we used, is from Cryogenics Ltd which needs the physical transfer of liquid helium in a regular interval. It can go from -9 to 9 T for various measurements. It is an RF SQUID which is based on AC Josephson effect.

FIGURE 2.5: SQUID based magnetometer

2.7 Tetra Arc Furnace

Tetra arc furnace is used to grow crystals of compounds that melt congruently. The sample is placed on a copper hearth in between four electrodes that use an electric arc to heat the sample uniformly from all four directions upon adjustment from the user. During the melting process, Argon environment is must to produce arc, so we use argon at a low pressure of 3 mbar. The argon gas provides an inert atmosphere that prevents the contamination of the sample. The copper puck is continuously cooled with flowing water at 17C to prevent copper from melting and contaminating the sample. Before heating the sample, a titanium getter was heated. Since at high temperatures, titanium can absorb oxygen, and this purifies the chamber further. Arc melting is usually used for compounds that

have relatively high conductance. The sample gets heated due to the amount of high current passing through it.

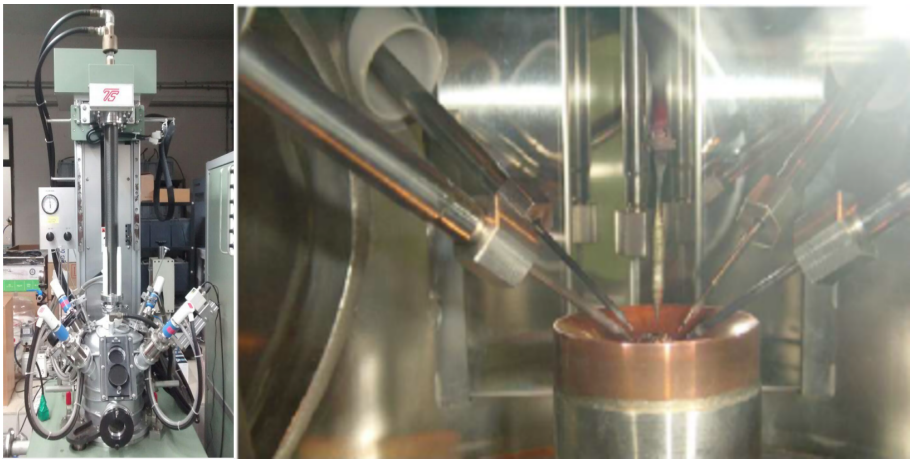

FIGURE 2.6: Tetra Arc Furnace[20]

2.8 Electron Dispersive X-Ray Spectroscopy

It is famously known as EDX or EDS. It is an analytical technique used for the elemental analysis or chemical characterization of a sample. A high energy beam of electrons are focused into the sample. Sample has electrons in discrete energy levels . The incident beam excites an electron of an inner shell and creating an electron whole. An electron from outer shell then comes and fills the cavity. The difference in energy between these two shells may be released in form of X-rays. These X-rays are measured by spectrometer and give us the name of the element from where signals are coming. Hence it confirms the presence of different atoms in a sample. It works well above detection of atoms with atomic number more than 6.

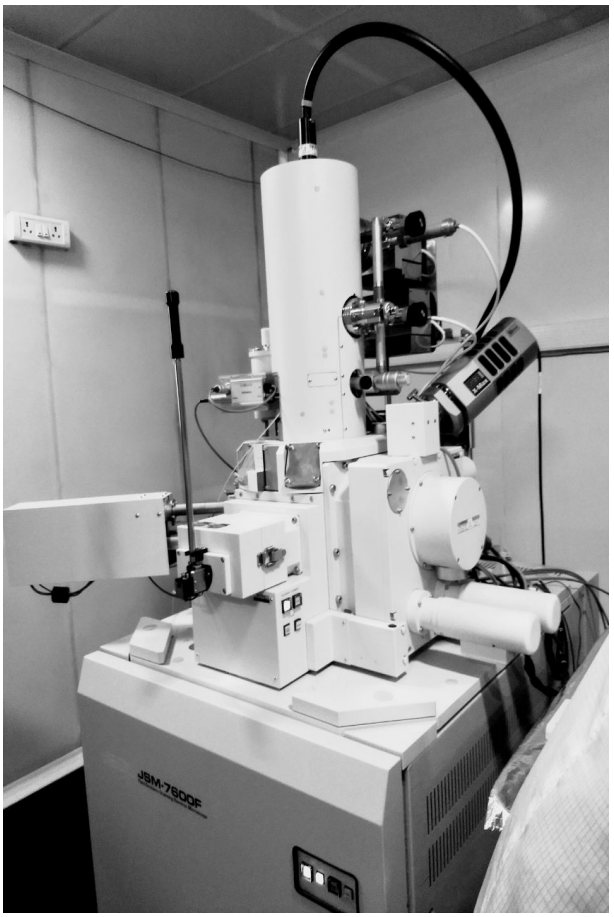

FIGURE 2.7: FE-SEM EDX

2.9 Crystal Growth and Synthesis

2.9.1 Crystal Growth of $RuCl_3$

$RuCl_3$ was prepared by self-flux growth method using high purity anhydrous Ruthenium(III) Chloride powder from Alfa Aesar. The stoichiometric amount was taken and vacuum sealed in quartz tube with V-shape at the end of the tube. It was then kept in a high-temperature table top furnace, which is made by Nabertherm, Germany. The maximum temperature was 1075°C and then slow cooling (@2°C/hr) was set. After this, it was quenched with normal tap water at 600°C in vertical position. Black layered crystals were seen at the bottom which was taken out and kept in argon environment inside the glove box.

2.9.2 Synthesis of $IrBr_3$

Around 400 mg of $IrBr_3.xH_2O$ power was taken and kept in a quartz tube. It was given 2-4 hours prolonged heating in boiling water to ensure complete dryness of powder. Roughing pump was running throughout the treatment with boiling water. After that, it was flushed three times with Ar gas and then sealed in the vacuum. It was kept in a box furnace in the vertical position. We have set up a cooling point inside the furnace by flowing chilled water through a copper pipe. We set the temperature to 750°C in the first trial, it did not melt then we checked at 1000°C, again it did not melt. We went maximum up to 1043°C and cooled down with a rate of 2°C/hr and quenching at 600°C. It could not melt even at that temperature.

We repeat the experiment without the water flow setup and checked at 750°C, it did not melt, again checked at 850°C, it did not melt. Temperature was then increased to 875°C, but it could not melt even at this temperature. Somehow the tube got broke this time, and we followed the following profile for next trial growth:

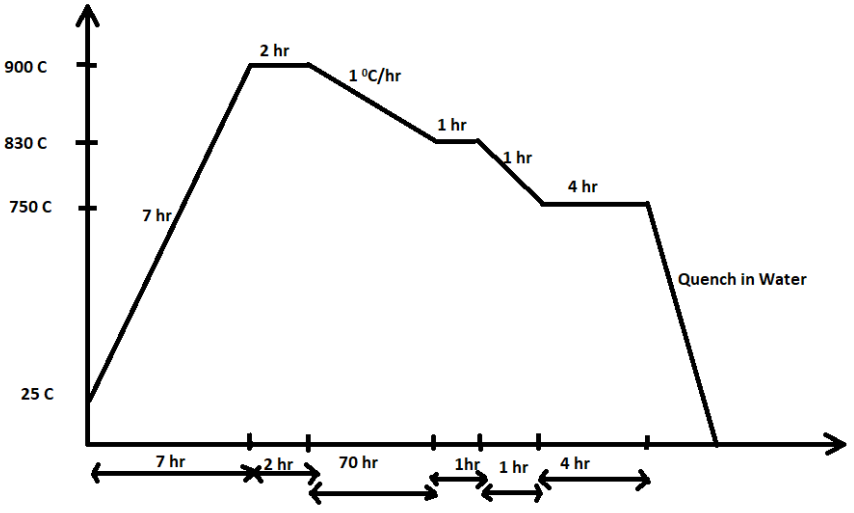

FIGURE 2.8: Temperature profile set to grow $IrBr_3$ crystals

2.9.3 Crystal Growth of $RuCl_3$ - $IrBr_3$ system

We attempted to grow α-$Ru_{0.95}Ir_{0.05}Cl_{2.95}Br_{0.05}$. Stoichiometric amounts of powders were taken and the total weight of the sample was taken to be around 400 mg. It was given 4 hour boiling water treatment to ensure complete dryness of sample inside the quartz tube. It was then sealed in vacuum and kept in a box furnace with maximum set temperature 1075°C, similar to $RuCl_3$ case. However, due to some reason, furnace got switched off around 850°C and then there was natural cooling till room temperature. Crystals could be seen at the top of the tube which has grown apparently due to vapour transport. At the bottom, some powders could be seen which could not form crystals. Crystals were taken out carefully and kept in the glove box.

2.9.4 Crystal Growth of $RuCl_3$-$RuBr_3$ system

It was grown by self-flux growth method. Both powders were taken in stoichiometric amounts and mixed thoroughly inside the Argon filled glove box. It was then kept in a quartz tube and given heat treatment through boiling water for 3 hours. Roughing Pump was on throughout the heating by boiling water. After giving sufficient time for drying, it was flushed three times with Argon and then sealed in the vacuum. Due to insufficient size of the sealed tube, it got broke two times in past so, this time a longer tube of length around 6cm was sealed and kept in a box furnace. Maximum temperature it went was 1000°C and then the cooling rate at 3°C/hr and water quench at 600°C in a vertical condition.

2.9.5 Crystal Growth of OsB_2

It melts congruently. So, It was grown by arc melting method in Tetra Arc Furnace of Techno Search. Metallic powder Os (99.95%, Alfa Aesar) was first made pellete as powders have a tendency to fly off if direct arc in applied on it and few chunks of Boron was kept below the Os pellete at tetra arc hearth. The copper hearth was cooled with continuous water flow at 17°C. Titanium was used as a getter to absorb all remaining Oxygen present in the vacuum chamber.

The sample was flipped and melted 7-10 times to ensure homogeneous mixing. Any loss of weight after melting was compensated by adding the required amount

of boron and again melted. This made many small mass samples and at the final stage, all were melted together to make a big poly crystal which was then planned to use for crystal pulling.

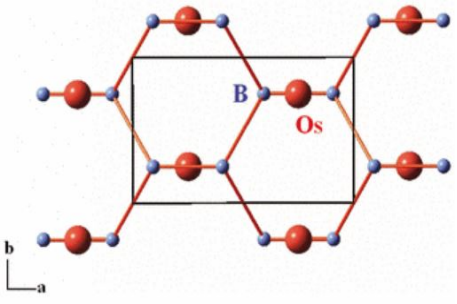

FIGURE 2.9: OsB_2 crystal structure viewed at the slight angle from the b axis. Os atom is shown by large red sphere while small blue sphere shows B atom[22]

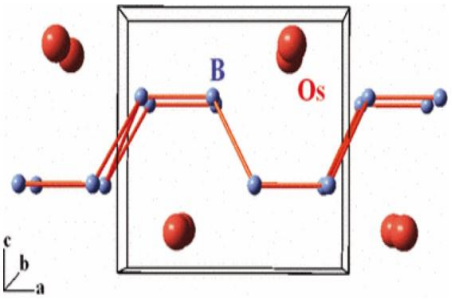

FIGURE 2.10: A projection of OsB_2 crystal structure onto the ab plane[22].

2.9.6 Crystal Growth of OsB_2-RuB_2 system

It was grown using tetra arc furnace. Already grown RuB_2 and $OsB_2$was used to make the poly crystal of composition $0.95OsB_2+0.05RuB_2$. It was melted 7-10 times and flipped after each melt to ensure homogeneous mixing.

Chapter 3

Characterization and Measurements

3.1 $RuCl_3$

3.1.1 EDX

Electron dispersive X-ray(EDX) measurements were performed at 25keV and 30keV energy. From the EDX measurements, stoichiometry of the compound $RuCl_3$ is confirmed. Crystal was clean and Ru:Cl was coming either exactly 25:75 or very little divergence in most of the case when checked with different crystals and it was uniform all over the surface.

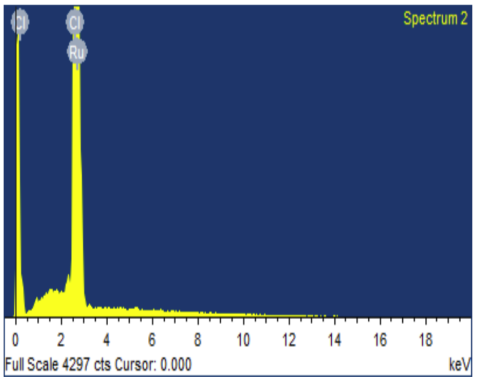

Element	Weight%	Atomic%
Cl K	51.28	75.00
Ru L	48.72	25.00
Totals	100.00	

FIGURE 3.1: $RuCl_3$ EDX spectra, It shows the amount of Ru and Cl in the crystal which is coming exactly what was expected. Right panel lists the found atoms in the crystal and their proportion

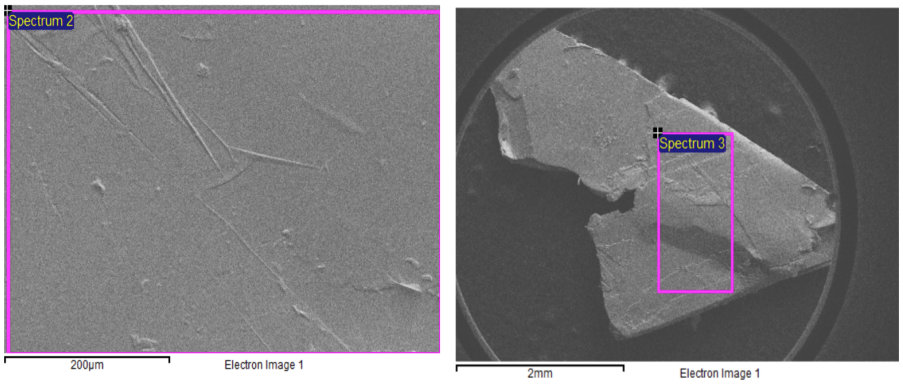

FIGURE 3.2: $RuCl_3$ crystal images during EDX. Crystals look clean and flat. $RuCl_3$ crystallizes in flat layers which can be seen over here

3.1.2 Magnetic Measurements

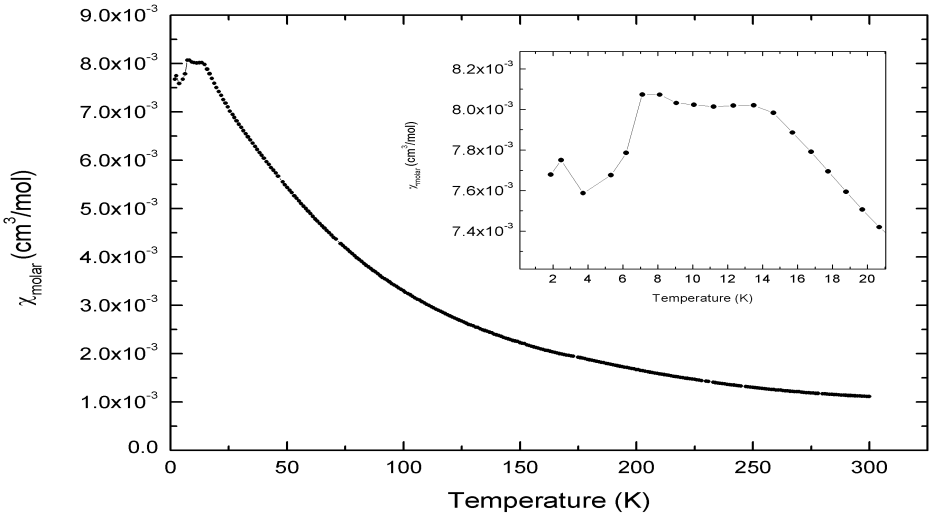

FIGURE 3.3: Molar susceptibility of a α-$RuCl_3$ single crystal is measured at 1T field applied parallel to ab plane. The ordering temperature was found to depend on the stacking order [4, [4] A.Banerjee, Nat Mater, vol. 15, pp. 733 740, Jul 2016] with two-layer periodic regions ordering at around 14 K and three layer periodic regions ordering at around 7 K. Inset is zoomed view of susceptibility and shows two transitions, one at 7.1 K and another at 13.5 K . This indicates the presence of a considerable amount of stacking faults in the measured crystal.

inv mom refined.png inv mom refined.png inv mom refined.bb inv mom refined.bb

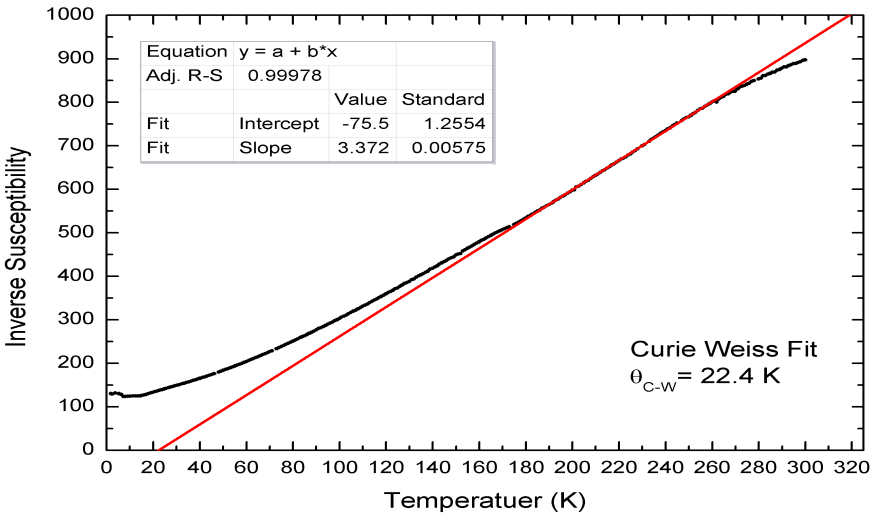

FIGURE 3.4: Magnetic Inverse susceptibility of α-$RuCl_3$ and its Curie-Weiss Fit is shown, which shows Curie-Weiss temperature of 22.4K

Magnetic measurements revealed long ranged magnetic ordering instead of the QSL state expected for a purely Kitaev magnet. Two transition point can be seen, one at 14K and another at 7K. The double transition is due to the presence of both kind of stacking faults in the sample of ABAB type and ABCABC type. Which means the measured sample is not very pure.

3.2 $IrBr_3$

$IrBr_3$ was reported to have monoclinic $C2/m$ space group and stacking of honeycomb layers like $RuBr_3$. It has structural similarity with $AlCl_3$[21] and by analogy its crystals may be another candidate of QSL. To explore this possibility, we tried to make its crystal through self-flux growth method.

3.2.1 Powder-XRD

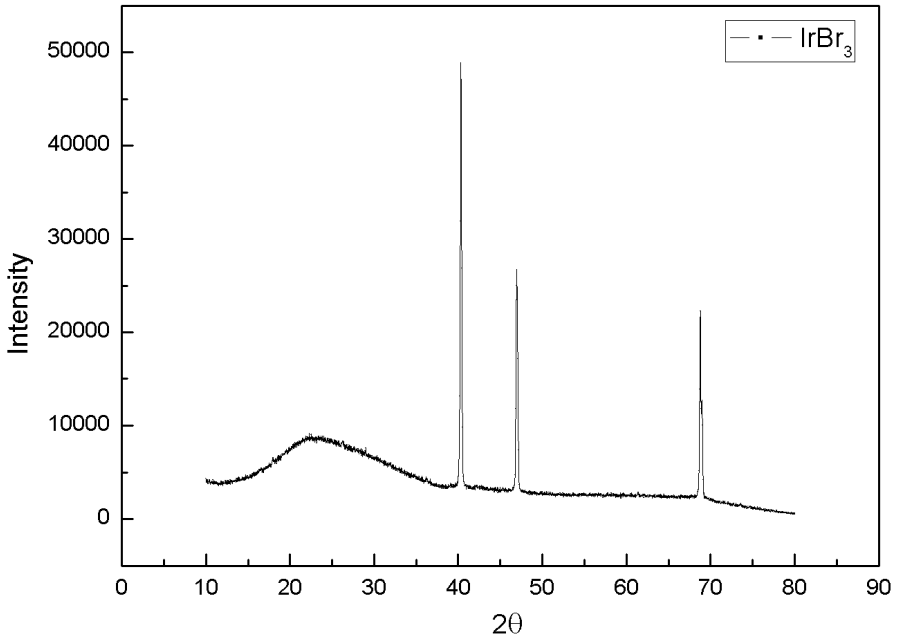

FIGURE 3.5: Powder XRD pattern of $IrBr_3$ powder after trial of crystal growth. only three peaks suggests a phase purity of poly crystals

We could not grow the crystal. It appeared that the powder did not melt even after repeating at 950°C. Powder XRD reveals that there are not so many phases but one. We did not try further growth attempts on this material.

3.3 $RuCl_3$ - $IrBr_3$ system

We have seen earlier that $RuCl_3$ and $IrBr_3$ has structural similarity. While $RuCl_3$ is a Kitaev candidate, we tried to dope Ir in the position of Ru and Br in the position of Cl in parent compound $RuCl_3$ in the hope of finding a new candidate for Kitaev material.

3.3.1 Crystal Images

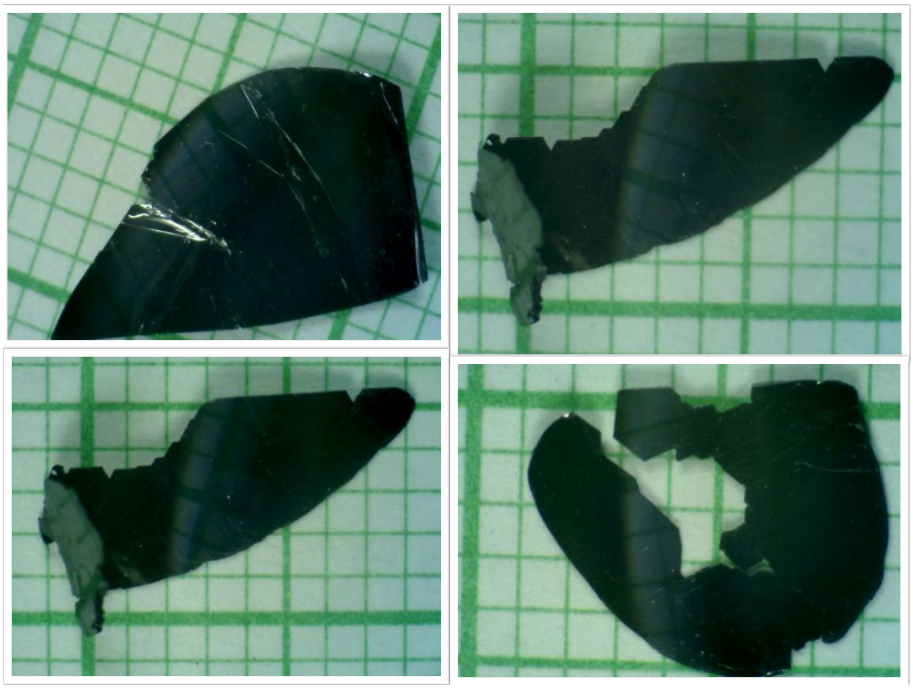

FIGURE 3.6: Big crystals of Br doped $RuCl_3$. Presence of Iridium could not be confirmed through EDX in the crystals.

3.3.2 EDX

EDX measurements were done at 30keV energy, and Br content was found in every crystal. Point and Area scan both were done for each crystal. Few bags of dust-like particles are seen at the surface of the crystal, so it was cleaved using Scotch tape, and then EDX was done in next round.

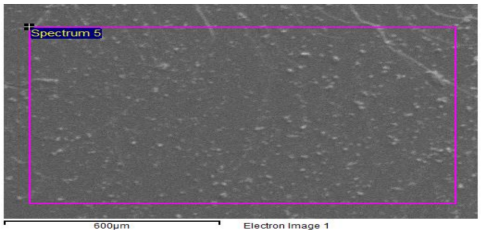

Element	Weight%	Atomic%
Cl K	48.68	72.64
Br K	3.54	2.34
Ru L	47.78	25.01
Totals	100.00	

FIGURE 3.7: EDX image of crystal and table on the right shows the 9% doping of Br into the crystal

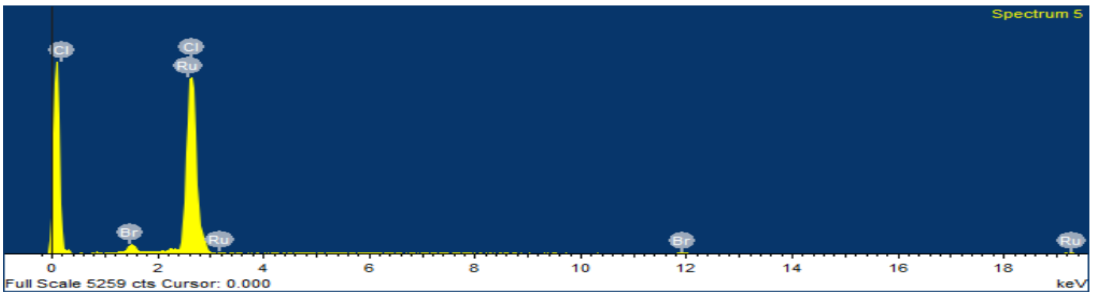

FIGURE 3.8: EDX spectra of 9% Br doped crystal, energy was set to 30keV

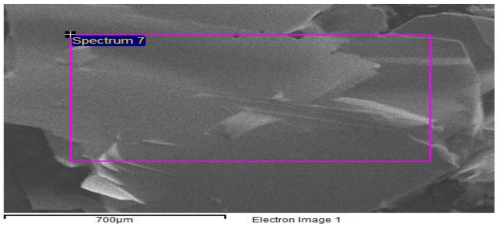

Element	Weight%	Atomic%
Cl K	50.50	74.10
Br K	3.04	1.98
Ru L	46.46	23.92
Totals	100.00	

FIGURE 3.9: EDX image of 7.8% of Bromine doped Crystal. Top surface of crystal was cleaved using Scotch tape

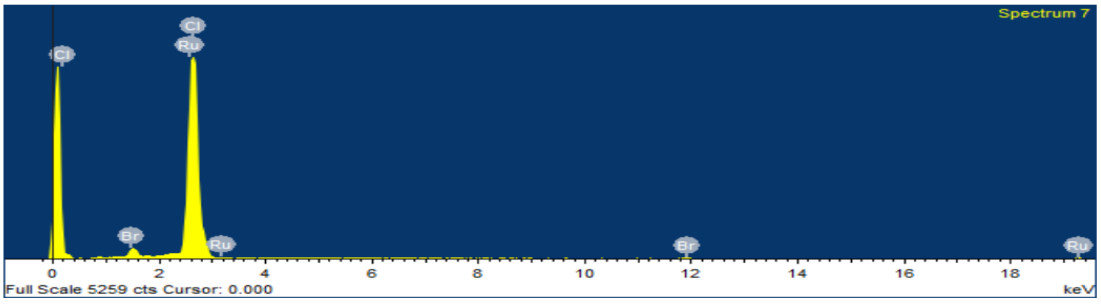

FIGURE 3.10: EDX spectra of 7.8% Br doped crystal, energy was 30keV

3.3.3 Magnetic Measurements

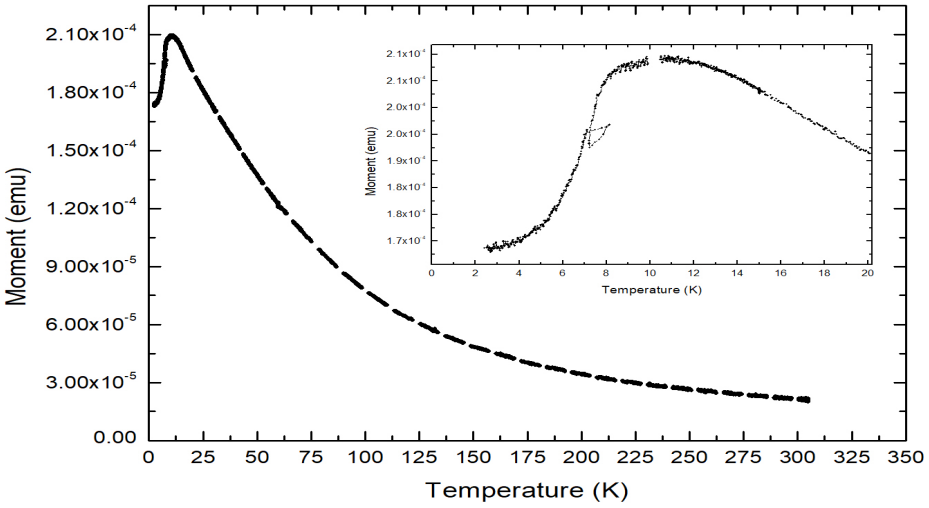

FIGURE 3.11: Susceptibility of $RuCl_{3-x}Br_x$ single crystal is measured at 1T field applied parallel to ab plane. Inset shows the zoomed view at low temperature.It shows double transition behavior like $RuCl_3$ but not very sharp transition points indicating not very good crystals

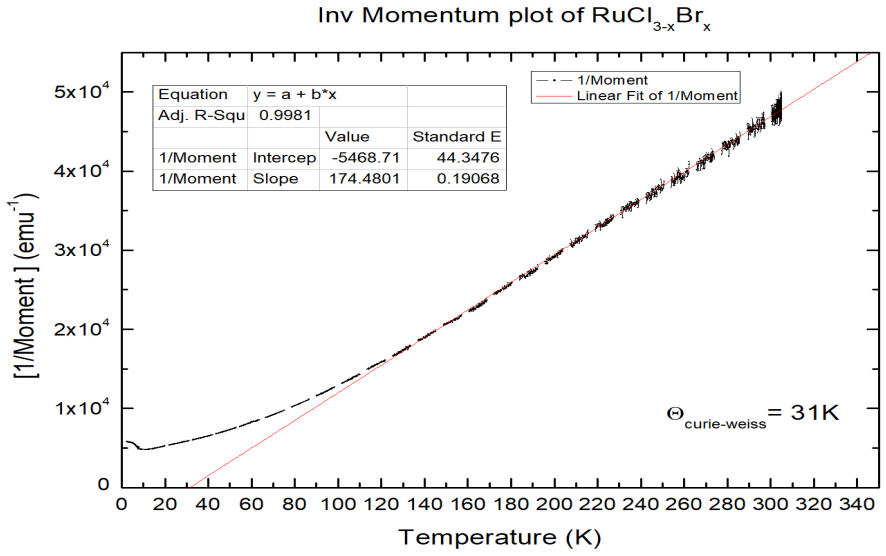

FIGURE 3.12: Inverse Susceptibility of the same $RuCl_{3-x}Br_x$ and Curie-Weiss fit gives Curie Weiss temperature=31K

Susceptibility measurement shows that the transition could survive with Bromine doping. We got many crystals of different doping, but we could not find any crystal with Ir content. So, only crystals with Bromine doping could be formed in layered thin flat form. Inverse susceptibility shows anti-ferromagnetic bulk ordering. We tried to grow crystals with 10% doping of Br but we could succeed in getting crystals with 9%, 6%, 5% Br doping etc.

3.4 $RuCl_3$-$RuBr_3$ crystal system

$RuBr_3$ has structural similarity with α-$RuCl_3$. We want to study the evolution of properties with doping of Bromine at place of Cl.

3.4.1 EDX

Bromine content is confirmed in powder through EDX and on the strip crystals, Bromine was there but some white dust was also present which had only Ru and Cl content.

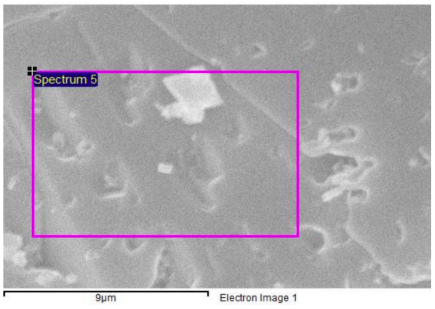

Element	Weight%	Atomic%
Cl K	50.36	73.95
Br K	3.56	2.32
Ru L	46.08	23.73
Totals	100.00	

FIGURE 3.13: EDX image of $RuCl_{2.9}Br_{0.1}$ powder and table on the right shows bromine doping of 9%

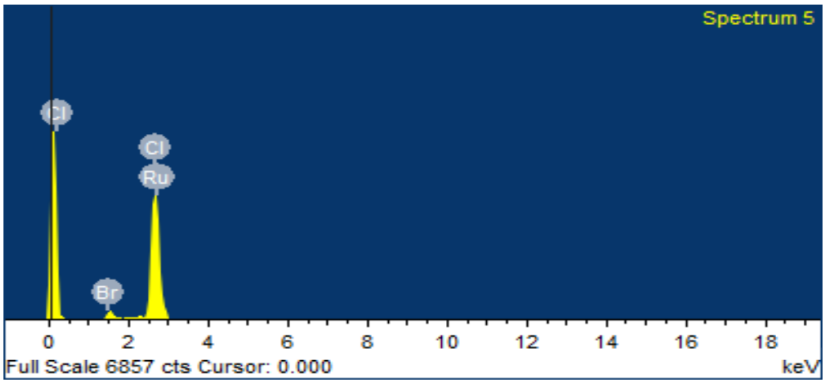

FIGURE 3.14: EDX spectra for powder sample of 9% Br doping

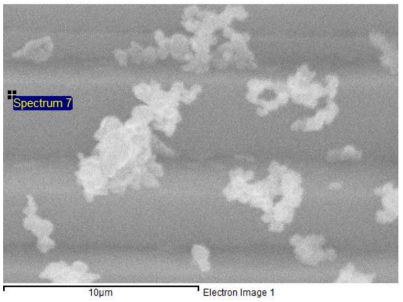

Element	Weight%	Atomic%
Cl K	49.92	73.82
Br K	1.46	0.96
Ru L	48.63	25.22
Totals	100.00	

FIGURE 3.15: EDX of long stripe crystal which was found at the wall of quartz tube and having 3% of Br doping

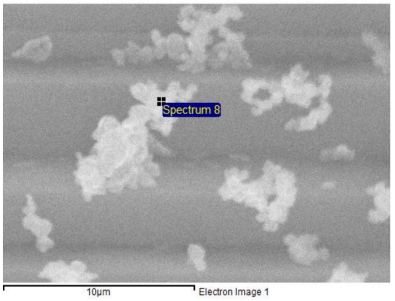

Element	Weight%	Atomic%
Cl K	35.33	60.90
Ru L	64.67	39.10
Totals	100.00	

FIGURE 3.16: EDX of dust over stripe crystal which was found at the wall of quartz tube and having only Ru and Cl

3.4.2 Powder-XRD

polycrystalline sample was formed and strip crystals on the walls could be found. XRD was done on powder poly crystals. However peaks of PXRD could not even closer to parent α-$RuCl_3$ theoretical XRD pattern. but the transition is of the similar type seen in α-$RuCl_3$.

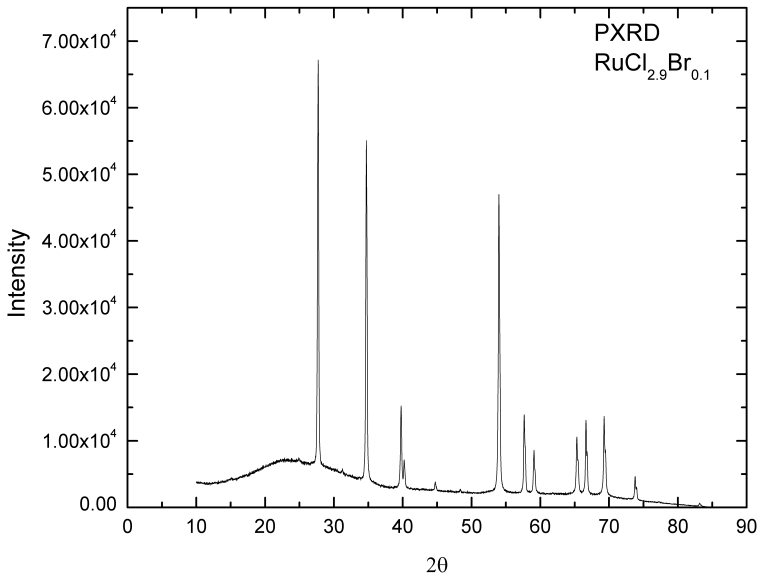

FIGURE 3.17: Powder XRD of poly crystalline sample

3.4.3 Magnetic Measurements

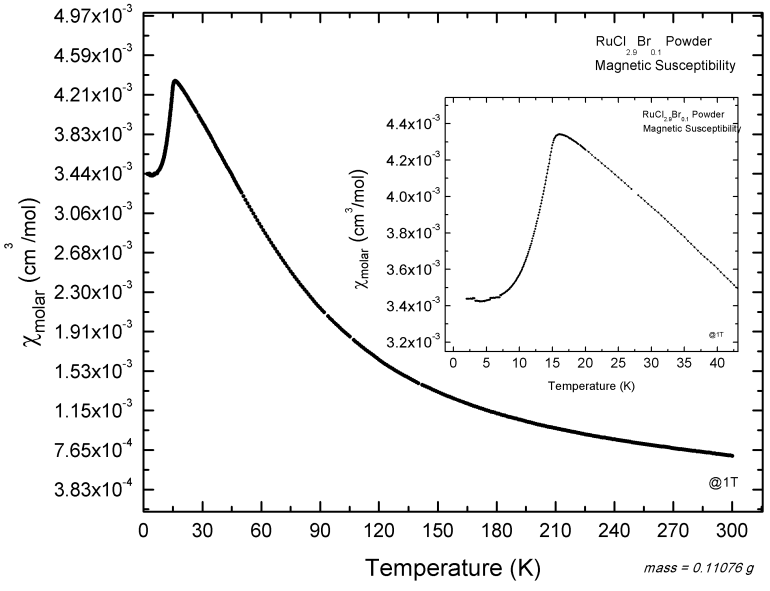

FIGURE 3.18: Molar Susceptibility of powder sample in SQUID based magnetometer, Despite having Br doping, transition could survives with ordering temperature around 15K

One transition was found around 15 K and it has a shift from α-$RuCl_3$ where it was around 14K. The transition is seen to survive even after Bromine doping. Strip crystals had stair-like structure and were thin. It was layered and strong. EDX showed the low bromine doping in strip crystals. The powder also showed bromine doping but nothing can be concluded about the doping in power case as it's XRD pattern did not match with original α-$RuCl_3$.

3.5 OsB_2

3.5.1 Images

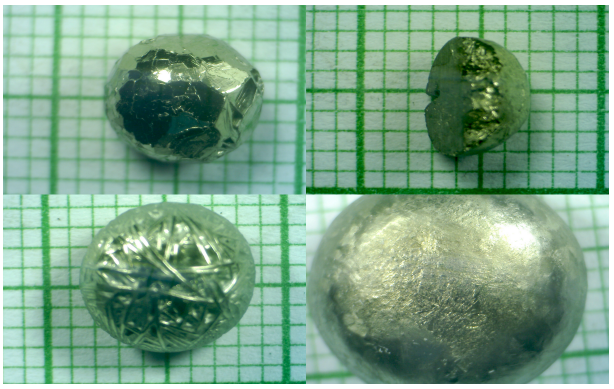

FIGURE 3.19: Images of OsB_2. Sample was cut using Diamond blade cutter to use for transport measurements.

3.5.2 EDX

It was hard to detect Boron in EDX. So, any data from EDX is not trustworthy. So, Resistivity measurement at PPMS was done to see the superconducting transition. It matched with already reported transition temperature[Yogesh Singh et al., PRB 82, 144532 (2010)].

3.5.3 Magnetic Measurements

Magnetic susceptibility measurement confirmed the transition temperature to be 2.1K, and thus it confirmed that the grown crystal is OsB_2. It also confirmed that all small crystals of OsB_2 was indeed OsB_2 and no ferromagnetic impurity could enter to the sample otherwise superconductivity would have destroyed in that case.

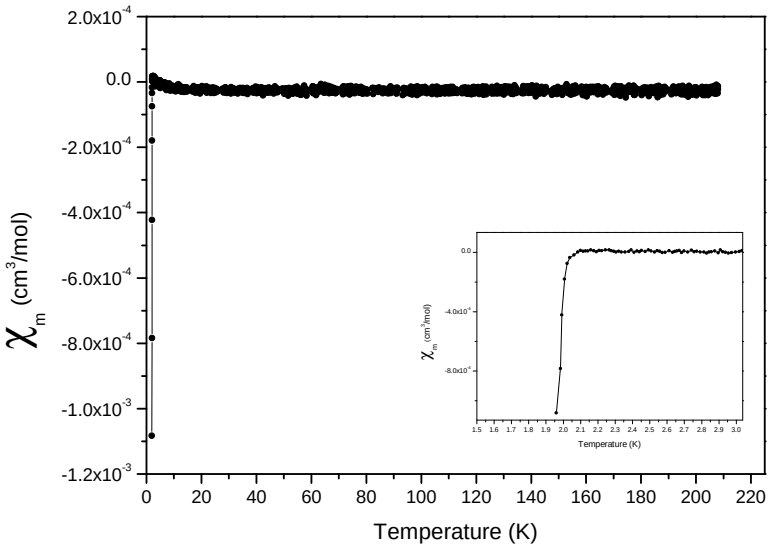

FIGURE 3.20: OsB_2 superconducting transition

3.6 OsB_2-RuB_2 system

$RuBr_3$ has structural similarity with $RuCl_3$. We want to study the evolution of properties with doping of Bromine at the place of Cl.

3.6.1 Images

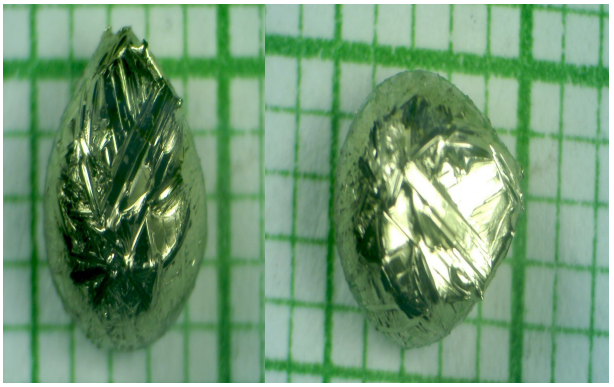

FIGURE 3.21: Images of $0.95OsB_2$+$0.05RuB_2$ poly crystals. Sample was grown in tetra arc furnace.

3.6.2 Transport Measurements

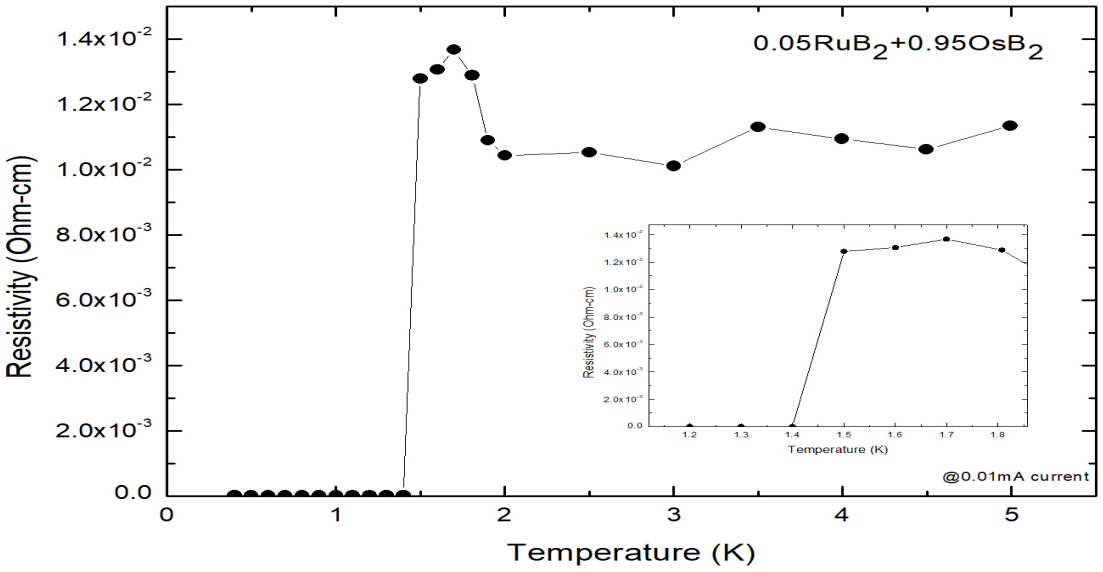

FIGURE 3.22: Resistivity was measured at a current of 0.01mA through four-probe method, and the superconducting transition survived with Ru doping and, superconducting transition point is 1.5K

Crystal of $0.95OsB_2$+$0.05RuB_2$ was grown successfully using tetra arc furnace. Resistivity measurement tells that it's transition temperature is 1.5K. A sudden jump in resistivity is seen below 2 K prior to superconducting transition. This behavior was not known earlier. However a clear decrease in transition upon Ruthenium doping can be seen.

Chapter 4

Discussion

The thesis is divided into two parts- study of α-$RuCl_3$ and OsB_2 compounds. Crystal growth of α-$RuCl_3$ and doped compounds were studied for magnetic properties. α-$RuCl_3$ is an excellent candidate in which Kitaev Physics can be explored. Although it orders magnetically nevertheless magnetic excitations shows its similarity with Kitaev spin liquid ground state. Despite the current work, a number of question remain unanswered. A detailed study of Bromine doping up to 60% need to be studied and not just bromine doping, but Cr doping at the site of Ru is also promising. $CrCl_3$ and CrI_3 has similarity with α-$RuCl_3$. So, the detailed study of the doped system could lead to the finding of more Kitaev like material.

OsB_2 and Ru doped OsB_2 need to be explored to understand the unusual superconducting behavior of this compound. A series of crystals of Ru doped OsB_2 need to be grown and studied.

Bibliography

[1] K. W. Plumb el al. Phys. rev. b, vol. 90, p. 041112. 2014.

[2] A.Kitaev. Annals of physics, vol. 321, no. 1, pp. 2 111, 2006.

[3] Yamada et al. Phys. rev. b 96, 155107.

[4] G. Jackeli et al. hys. rev.lett., vol. 102, p. 017205, jan 2009.

[5] Jennifer Sears. Thesis utoronto.

[6] S. Hwan Chun et al. at phys, vol. 11, pp. 462466, jun 2015. letter.

[7] Yogesh Singh et al. Phys. rev. b, vol. 82, p. 064412,aug 2010.

[8] Yogesh Singh et al. Phys. rev. lett., vol. 108, p. 127203, mar 2012.

[9] X.Liu et al. Phys. rev. b, vol. 83, p. 220403, jun 2011.

[10] Fletcher et al. . chem. soc. a, pp. 10381045, 1967.

[11] A.Banerjee et al. Nat mater, vol. 15, pp. 733740, jul 2016.

[12] H.B.Cao et al. Phys. rev. b, vol. 93, p. 134423, apr 2016.

[13] A.Banerjee et al. Science, vol. 356, no. 6342, pp. 10551059, 2017.

[14] L. J. Sandilands et al. Phys. rev. lett.,vol. 114, p. 147201, apr 2015.

[15] H.K.Onnes. $www.nobelprize.org/nobel_prizes/physics/laureates/1913/onnes-bio.html$.

[16] Cooper Bardeen and Schrieffer. $www.nobelprize.org/nobel_prizes/physics/laureates/1972/$.

[17] Carlstrom et al. Physical review b 83, 174509 (2011).

[18] A.Abrikosov. Sov. phys. jetp 5, 1174 (1957).

[19] PRL 2009 Moschalkov et al.

[20] $Source: M.SzlawskaandD. Kaczorowski.$

[21] Brodersen et al. Journal of the less-common metals.

[22] Yogesh Singh et al. Prb 82,144532 (2010).